

$T - \mu$ phase diagram of the chiral quark model from a large flavor number expansion

A. Jakovác^a, A. Patkós^{b,1}, Zs. Szép^c, P. Szépfalusy^{b,d,2}

^a *Hungarian Academy of Sciences and Budapest University of Technology and Economics,
Research Group “Theory of Condensed Matter”, H-1521 Budapest, Hungary*

^b *Eötvös University, H-1117 Budapest, Hungary*

^c *Research Group for Statistical Physics of the Hungarian Academy of Sciences,
H-1117 Budapest, Hungary*

^d *Research Institute for Solid State Physics and Optics, Hungarian Academy of Sciences,
H-1525 Budapest, Hungary*

Abstract

The chiral phase boundary of strong matter is determined in the $T - \mu$ plane from the chiral quark model, applying a non-perturbatively renormalised treatment, involving chains of pion-bubbles and 1-loop fermion contributions. In the absence of explicit symmetry breaking the second order portion of the phase boundary and the location of the tricritical point (TCP) are determined analytically. Sensitivity of the results to the renormalisation scale is carefully investigated. The softening of the σ -pole near the second order transitions is confirmed.

Key words: large N approximation, tricritical point, finite density

PACS: 11.10.Wx, 11.30.Rd., 25.75.Nq

1 Introduction

The chiral phase structure of QCD at nonzero quark density receives renewed interest with the advent of new lattice techniques [1,2,3,4,5,6]. Recent investigations concentrate on the transformation of the temperature driven crossover into first order transitions with increasing bario-chemical potential. In the present letter we shall address the same issue.

The lattice approach is an exact tool, but requires thorough investigation of finite quark mass and lattice spacing effects. In particular, the chiral limit with zero mass pions is

Email addresses: jakovac@planck.phy.bme.hu (A. Jakovác), patkos@ludens.elte.hu (A. Patkós), szepzs@antonius.elte.hu (Zs. Szép), psz@galahad.elte.hu (P. Szépfalusy).

¹ Department of Atomic Physics

² Department of Physics of Complex Systems

beyond the access of present numerical QCD techniques (see, however [7]). An interesting attempt for a “phenomenological” interpretation of lattice data in the hadronic phase was recently proposed. A hadronic resonance model with bag-motivated quark mass dependence of the hadron spectra describes fairly well the thermodynamics of lattice QCD with unnaturally heavy pseudoscalar mesons in the low temperature phase [8,9] (see also [10]).

Extensive literature exists on the phase structure of effective theories matched to phenomenological data. Following the pioneering work of Barducci *et al.* [11] detailed studies were published in Nambu-Jona-Lasinio models [12,13,14] and in the linear σ model [15,16,13].

These investigations do not go beyond some version of the quasi-particle approach, e.g. the thermodynamical potential is approximated by a sum of free particle contributions with masses obtained from some sort of selfconsistent gap equations. The renormalisation of the selfconsistent set of equations of state (EoS) and propagators represents a notoriously difficult problem. In particular in the broken phase the UV divergences of the selfenergies have temperature and μ -dependent coefficients, also depending on the chiral condensate. In general, subtraction of such terms defines oversubtracted renormalisation schemes. In higher orders of the perturbative solution one expects that resummed or improved expansions demonstrate the cancellation of the apparent temperature/ μ /condensate-dependent counterterms [17]. Despite promising recent progress [18,19] no general enough implementation is available to date for obtaining a renormalised set of equations in which resummed propagators could be used. Therefore it is hard to assess the accuracy of the predictions obtained from quasi-particle descriptions.

In the present letter we extend our recent treatment of the pure $O(N = 4)$ model in the approximation of large number of Goldstone bosons (N) [20] to the chiral quark model at finite μ . The effect of the constituent quarks will be represented in this letter by 1-loop contributions. We shall find fermion effects which are of $\mathcal{O}(1/\sqrt{N})$. A resummed renormalisation scheme will be proposed for the coupled set of EoS, and the π and σ propagators. Finally, the renormalised equations will be analysed in the chiral limit, with Goldstone’s theorem being consistently obeyed. Since $N = 4$ is only moderately large, the fermionic contributions will not be considered in the numerical solution as perturbations of the leading large N solution. They rather will be included fully into the equations, and we shall search for a new (non-iterative) solution. The phase boundary will be fully traced in the $T - \mu$ plane.

The parameters of the model will be fixed with reference to the $T = 0$ mass and width of the σ particle [21]. It turns out that the renormalisation scale influences very strongly the shape of the spectral function in the sigma channel. The reason for this phenomenon is found in the appearance of extra unphysical poles on the physical Riemann sheet in a certain range of the renormalisation scale. After restricting the investigation to the physically allowed region, we decided to scan through a large domain of the renormalisation scale with the aim to see the sensitivity of the phase boundary in the $T - \mu$ -plane to its choice. We find that $T_c(\mu = 0)$ is fairly close to the range of critical temperatures mea-

sured in two-flavor QCD with different fermion discretisations. The coordinates of TCP are in good qualitative agreement with its earlier determinations from effective models [13], implying $T_{TCP} \leq 70$ MeV independently of the renormalisation scale.

2 The model and its equation of state

In the definition of the model we display explicitly the flavor factors:

$$L[\sigma, \pi^a, \psi] = L_M[\sigma, \pi^a] + L_F[\sigma, \pi^a, \psi] + \delta L_{ct}[\sigma, \pi^a, \psi], \quad (1)$$

where

$$\begin{aligned} L_M = & - \left[\frac{\lambda}{24} \Phi^4 + \frac{1}{2} m^2 \Phi^2 \right] N - \left[\frac{\lambda}{6} \Phi^3 + m^2 \Phi \right] \sigma \sqrt{N} \\ & + \frac{1}{2} \left[\partial^\mu \sigma(x) \partial_\mu \sigma(x) + \partial^\mu \pi^a(x) \partial_\mu \pi^a(x) \right] - \frac{1}{2} m^2 \left[\sigma^2(x) + \pi^a(x) \pi^a(x) \right] \\ & - \frac{\lambda}{12} \Phi^2 \left[3\sigma^2(x) + \pi^a(x) \pi^a(x) \right] \\ & - \frac{\lambda}{6\sqrt{N}} \Phi \left[\sigma^3(x) + \sigma(x) \pi^a(x) \pi^a(x) \right] - \frac{\lambda}{24N} \left[\sigma^2(x) + \pi^a(x) \pi^a(x) \right]^2. \\ L_F = & \bar{\psi}(x) \left[i \partial^\mu \gamma_\mu - m_q - \frac{g}{\sqrt{N}} \left(\sigma(x) + i \sqrt{2N_f} \gamma_5 T^a \pi^a(x) \right) \right] \psi(x), \end{aligned} \quad (2)$$

$\delta L_{ct}[\sigma, \pi^a, \psi]$ is the counterterm Lagrangian. In the large N limit one has $N_f = \sqrt{N}$. The above form refers explicitly to the broken symmetry phase with the condensate giving rise also to the mass of the constituent fermion, which stays finite in the large N limit:

$$\sigma(x) \rightarrow \sqrt{N} \Phi + \sigma(x), \quad m_q = g \Phi. \quad (3)$$

It is noteworthy that the linear σ model has a second independent quartic coupling for $N_f > 2$, which we fix for simplicity at zero, since we wish to evaluate the expressions derived in the large N approximation for $N = 4$. Also, in this letter we work in the chiral limit, that is no explicit symmetry breaking term is introduced into the Lagrangian. The chemical potential for fermions is introduced into the fermionic piece of the Lagrangian by the replacement: $\partial_t \rightarrow \partial_t - i\mu$.

The form of EoS to $\mathcal{O}(1/\sqrt{N})$ with N_c colored quarks is the following:

$$\sqrt{N} \Phi \left[m^2 + \frac{\lambda}{6} \Phi^2 + \frac{\lambda}{6N} \langle \pi^a \pi^a \rangle_M \right] + \frac{g N_c}{\sqrt{N}} \langle \bar{\psi} \psi \rangle = 0. \quad (4)$$

It is obvious that the fermionic contribution is $\mathcal{O}(1/\sqrt{N})$. The fermion tadpole will be evaluated using the tree-level mass m_q . The subscript M at the expectation value of the composite operator $\bar{\pi}^2(x)$ refers to an effective pion tadpole computed with propagator mass

M , which sums the contribution of all super-daisy type diagrams [22]. The corresponding pion propagator is determined from the Schwinger-Dyson equation as $iG_\pi^{-1}(p^2 = M^2) = 0$:

$$iG_\pi^{-1}(p) = p^2 - m^2 - \frac{\lambda}{6}\Phi^2 - \frac{\lambda}{6N}\langle\pi^a\pi^a\rangle_M - B_{1\psi}(p). \quad (5)$$

Here $B_{1\psi}$ is the contribution of the fermionic bubble to the self-energy of the pion. By an algebraic transformation of its integrand it can be related to the fermionic tadpole as follows:

$$B_{1\psi}(p) = \frac{gN_c}{N\Phi}\langle\bar{\psi}\psi\rangle + \frac{2g^2N_c}{\sqrt{N}}p^2 I_F(p, m_q), \quad (6)$$

where $I_F(p, m_q)$ is the scalar bubble integral with external momentum p , but evaluated with the fermion mass and with Fermi-Dirac distribution, $f_F^\pm(\omega) = 1/(\exp(\beta(\omega \mp \mu)) + 1)$:

$$I_F(p, m_q) = I_F^0(p, m_q) - I_F^\beta(p, m_q), \quad (7)$$

$$I_F^0(p, m_q) = \int \frac{d^4k}{(2\pi)^4} \frac{i}{(k^2 - m_q^2 + i\epsilon)((k-p)^2 - m_q^2 + i\epsilon)}, \quad (8)$$

$$I_F^\beta(p, m_q) = \int \frac{d^3k}{(2\pi)^3} \frac{1}{4\omega_1\omega_2} \left[\frac{f_F^+(\omega_1) + f_F^-(\omega_2)}{p_0 - \omega_1 - \omega_2 + i\epsilon} - \frac{f_F^-(\omega_1) + f_F^+(\omega_2)}{p_0 + \omega_1 + \omega_2 + i\epsilon} \right. \\ \left. - \frac{f_F^+(\omega_1) - f_F^-(\omega_2)}{p_0 - \omega_1 + \omega_2 + i\epsilon} + \frac{f_F^-(\omega_1) - f_F^+(\omega_2)}{p_0 + \omega_1 - \omega_2 + i\epsilon} \right]. \quad (9)$$

Substituting (6) into (5) and making use of (4) one finds that for $p^2 = 0$ the inverse propagator vanishes. This means that Goldstone's theorem is fulfilled and a zero mass pion can be used consistently for the evaluation of the pion tadpole in (4).

Next, we evaluate EoS, for instance, with dimensional regularisation. After \overline{MS} subtraction, which corresponds to a perturbative renormalisation of λ with a counterterm proportional to g^4 , one arrives for EoS at

$$m^2 + \frac{\lambda}{6}(\Phi^2 + T_B(0)) - \frac{4g^2N_c}{\sqrt{N}}T_F(m_q) = 0, \quad (10)$$

where $T_a(x)$, $a = B, F$ stands for the bosonic/fermionic tadpole contribution with mass x :

$$T_a(x) = \frac{x^2}{16\pi^2} \ln \frac{ex^2}{M_{0a}^2} - T_a^\beta(x), \quad T_a^\beta(x) = \frac{1}{2\pi^2} \int_x^\infty d\omega \sqrt{\omega^2 - x^2} f_a(\omega), \\ f_F(\omega) = \frac{1}{2} [f_F^+(\omega) + f_F^-(\omega)], \quad f_B(\omega) = \frac{1}{e^{\beta\omega} - 1}. \quad (11)$$

Here M_{0a} are the renormalisation scales, which can be chosen different for the fermionic and the bosonic tadpoles. Below we shall characterize the relationship of the two scales by

$\eta = \ln(M_{0B}/M_{0F})$, which introduces an extra finite subtraction into the renormalisation scheme. We shall check if substantially different phenomenology can be achieved when this freedom is exploited.

3 Analytical determination of the TCP

When looking for the location of continuous phase transitions in the $T - \mu$ plane, one can study the left hand side of (10) for small field values and in power series of the fugacity, $\exp(\mu/T)$. One expands the distribution function for fermions and antifermions in power series, and changes the order of the integration and the summation, doing the integration first. One expands the resulting modified Bessel functions up to linear order in m_q and eventually performs the remaining sum. Remarkably, the logarithmic dependence on Φ is cancelled, and a power series in Φ is the result. The sign for a continuous phase transition, the vanishing of the constant term is given (after substituting $N = 4$) by the equation

$$m^2 + \frac{\lambda}{72}T_c^2 - \frac{g^2T_c^2}{2\pi^2}N_c \left(Li_2(-e^{\mu/T_c}) + Li_2(-e^{-\mu/T_c}) \right) = 0. \quad (12)$$

In particular for $\mu = 0$ one finds a shift downwards in T_c due to the fermionic fluctuations:

$$m^2 + \left(\frac{\lambda}{72} + \frac{g^2N_c}{12} \right) T_c^2 = 0. \quad (13)$$

For small μ the coefficient of the quadratic part is positive, therefore T_c is consistently interpreted as a critical point. The second order line ends at $T = T_{TCP}$, $\mu = \mu_{TCP}$, where also the quadratic coefficient changes sign:

$$\frac{\lambda}{6} + \frac{g^4N_c}{4\pi^2} \left[\frac{\partial}{\partial n} \left(Li_n(-e^{-\mu_{TCP}/T_{TCP}}) + Li_n(-e^{-\mu_{TCP}/T_{TCP}}) \right) \right]_{n=0} - \ln \frac{cT_{TCP}}{M_0B} = 0, \quad (14)$$

($\ln(c/2) = 1 - \gamma_E + \eta$). The first order line for larger μ values was determined numerically directly from (10). Also the perfect agreement of the semi-analytically determined second order portion of the phase boundary with the exact one was verified numerically.

The parameters λ , g , Φ , M_{0a} , m^2 should be determined from the $T = 0$ data. One requires the EoS to give $\Phi = f_\pi/2$, with $f_\pi = 93$ MeV. Then the value of $m_q(T = 0) \equiv m_{q0}$ determines g . We have chosen $m_{q0} = m_N/3 \approx 312.67$, so that $g = 6.72$. The EoS at $T = 0$ provides one relation among m^2 , λ and the renormalisation scales M_{0a} , from which m can be determined once the other three parameters are known. One would like to fully fix these three parameters M_{0a} and λ , for instance, by studying the spectroscopy of the σ particle [20]. The relationship between the pole and the spectral function will be discussed in section 4. Here we elaborate on the features of the phase boundary when scanning through a large domain of M_{0B} and η for fixed value of $\lambda = 400$.

In Fig.1 (l.h.s.) the dependence of the critical temperature on M_{0B} is shown at $\mu = 0$ for

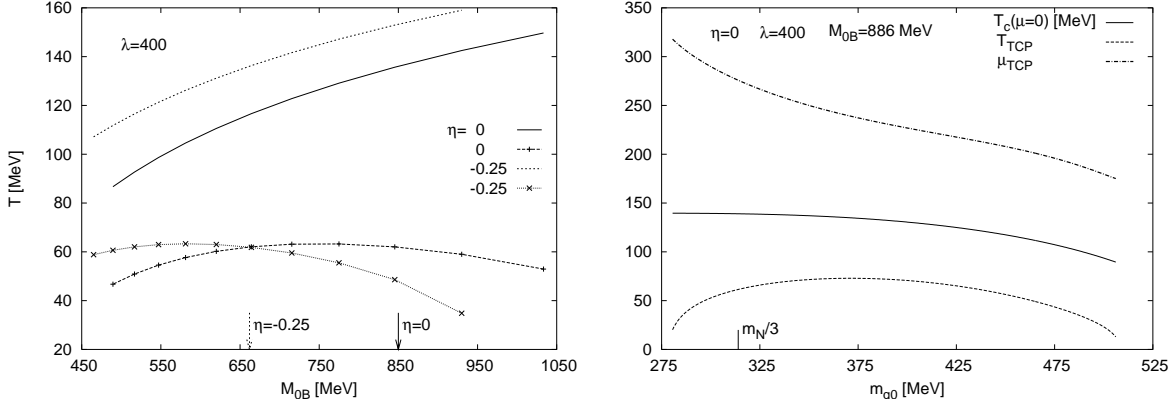


Fig. 1. L.h.s.: the variation of $T_c(\mu=0)$ (upper curves) and of T_{TCP} (lower curves) with M_{0B} for $\eta=0$ and -0.25 (for the definitions see the text). The arrows on the abscissa separate the region of stable (right) and unstable (left) solutions for different values of η . R.h.s.: the dependence of $T_c(\mu=0)$, T_{TCP} and μ_{TCP} on the constituent quark mass m_{q0} .

$\eta=0, -0.25$. It should be emphasized that by the arguments to be presented in Section 4 the allowed range of M_{0B} lies to the right from the arrow, appearing on the horizontal axis of the figure. It is clear that in this region one can arrange very easily $T_c(\mu=0)$ to occur in the region 150-170 MeV, where it is indicated by lattice studies of the two flavor QCD with dynamical quarks [23,24]. The temperature of the tricritical point changes very mildly and stays for all choices below 70 MeV. Another informative representation of the phase structure is to display the dependence of $T_c(\mu=0)$, T_{TCP} and μ_{TCP} on the constituent quark mass, which appears on the r.h.s. of Fig. 1.

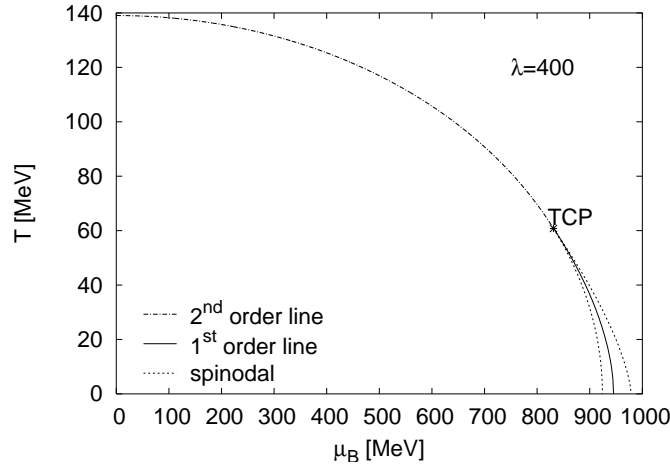


Fig. 2. The $T - \mu$ phase diagram in the chiral limit for $M_{0B} = 886$ MeV and $\eta = 0$.

We draw the complete phase diagram in Fig. 2 with $m_{q0} = m_N/3$ and $\eta = 0$ for $M_{0B} = 886$ MeV. The left spinodal is simply the continuation of the second order phase boundary, the right spinodal is found by locating the turning point of the two-valued order parameter curve as a function of μ for fixed T . We notice that the metastable region between the spinodal curves becomes narrower with increasing M_{0B} . In between we draw the phase boundary by finding the degeneracy point of the thermodynamical potential. When com-

pared with the features of the previous (non-renormalised) investigations in effective models [13], one realizes that the theoretical consistency achieved in the present treatment does not produce qualitative differences. If we tune η in such a way that $T_c(\mu = 0)$ increases then TCP moves further down and rightwards on the phase diagram. Our phase boundary drops much steeper than the present lattice estimates [6] performed with rather heavy quarks and is quite close to the freeze-out curve of Cleymans and Redlich [25].

4 Poles in the σ channel and their relation to the spectral function

In the present letter we need the spectral function in the σ channel only for $T = 0$, that is for discussing the sensitivity of its pole structure to the selection of the couplings, especially the renormalisation scales of the effective model. A detailed analysis of the features of the finite temperature pole trajectory and the phenomenon of the threshold enhancement is postponed to a forthcoming publication. The large N form of the inverse propagator of the σ particle [20] is now modified by the contribution of the fermionic loop:

$$iG_\sigma^{-1}(p) = p^2 - m^2 - \frac{\lambda}{2}\Phi^2 - \frac{\lambda}{6N}\langle\pi^a\pi^a\rangle_M - S_{chain}(p) - \frac{gN_c}{N\Phi}\langle\bar{\psi}\psi\rangle + \frac{2g^2N_c}{\sqrt{N}}(4m_{q0}^2 - p^2)I_F(p, m_{q0}) + \text{counterterms}. \quad (15)$$

Here $S_{chain}(p)$ represents the sum of the infinite sequence of pion bubble contributions to the σ self energy. This equation simplifies if (4) is taken into account to

$$iG_\sigma^{-1}(p) = p^2 - \frac{\lambda}{3}\Phi^2 - S_{chain}(p) + \frac{2g^2N_c}{\sqrt{N}}(4m_{q0}^2 - p^2)I_F(p, m_{q0}) + \text{counterterms}. \quad (16)$$

Fermionic counterterms are needed for the perturbative renormalisation of the coefficients of p^2 and of Φ^2 , both receiving divergent contribution from $I_F(p, m_{q0})$. Using \overline{MS} subtraction the fermionic part of the coupling constant counterterm which is $\mathcal{O}(g^4)$, proves to be the same as the one encountered in the renormalisation of the EoS. Additional bosonic counterterms form a power series in λ , and are needed to renormalise the chain of bubbles S_{chain} . This series can be formally resummed, resulting in a non-perturbative renormalisation of the meson sector [20]. The relation between the bare and renormalised coupling constant is:

$$\lambda_{\text{bare}} = \frac{\lambda}{1 + \frac{\lambda}{6}b_{div}} + \frac{24g^4}{\sqrt{N}}b_{div}, \quad b_{div} = \frac{1}{16\pi^2} \left(-\frac{1}{\epsilon} + \gamma - 2 - \ln(4\pi) \right). \quad (17)$$

Summing up the renormalised terms of the bubble chain, the final renormalised σ propa-

gator at rest ($\mathbf{p} = 0$) reads as follows:

$$iG_\sigma^{-1}(p_0, 0) = p_0^2 - \frac{\lambda}{3}\Phi^2 \left(1 - \frac{\lambda}{6}I_{B,R}(p_0, 0)\right)^{-1} + \frac{2g^2 N_c}{\sqrt{N}}(4m_{q0}^2 - p_0^2)I_{F,R}(p_0, m_{q0}). \quad (18)$$

The spectral function is obtained by putting $p_0 \rightarrow p_0 + i\epsilon$, and taking the imaginary part along the physical real axis:

$$\rho_\sigma(p_0) = \frac{1}{\pi} \text{Im} [iG_\sigma(p_0 + i\epsilon, 0)]. \quad (19)$$

Below we explore how the σ pole structure in the lower halfplane is reflected in the shape of the spectral function for a broad range of the values of the renormalisation scale M_{0B} as it appears in Fig. 1. An analytic continuation of (18) is understood via the $T = 0$ expressions of $I_{a,R}$, which for complex values of p_0 can be written explicitly as

$$\begin{aligned} I_{B,R}^0(p_0, 0) &= \frac{1}{16\pi^2} \left[\ln \frac{p_0^2}{M_{0B}^2} - ik_1\pi \right] \\ I_{F,R}^0(p_0, m_{q0}) &= \frac{1}{16\pi^2} \left[\ln \frac{m_{q0}^2}{M_{0F}^2} - Q \left(\ln \frac{1-Q}{1+Q} + ik_2\pi \right) \right], \quad Q = \sqrt{1 - \frac{4m_{q0}^2}{p_0^2}}. \end{aligned} \quad (20)$$

The above formulae correspond to analytical continuations onto specific Riemann-sheets characterised by two integers (k_1, k_2) . For example $k_1 = 1, k_2 = 1$ and $k_1 = 1, k_2 = -1$ corresponds to an analytical continuation across the real axis above and below the two-fermion threshold, respectively. We found roots of the right hand side of (18) for all $k_1 > 0, k_2 < 0$ integers. For a wide range of λ values the real parts of all poles have nearly the same value and lie slightly below the two-quark threshold. Therefore one expects the spectral function to have the maximum of its "resonant" part at $p_{0,max} \approx \text{Re}(p_{0,pole})$.

This expectation turned out to be incorrect below certain values of the renormalisation scale, depending on η . What spoils this feature is the Landau pole structure on the first Riemann sheet, which is an indication of the effective nature of the theory. This structure sensitively depends on M_{0B} . Apart from the well known large scale Landau pole(s) on the imaginary axis, which decreases exponentially with increasing values of λ , new small scale poles might emerge.

The mechanism for their occurrence is the cleanest to illustrate for $\lambda = 0$. In this case the imaginary part of a physical σ pole necessarily vanishes. For $M_{0B} > M_{0L}$ the pole is real but its location shifts towards the origin as M_{0B} decreases. At $M_{0B} = M_{0L}$ it reaches the origin and collides with its mirror arriving along the real axis from the direction $p_0 < 0$. For $M_{0B} < M_{0L}$ a conjugate pair of poles appears along the imaginary axis. One of them signals the instability of the system at very low energy scales, completely invalidating our solution in this region of the renormalisation scales. This dipole induced instability prevails also for $\lambda = 400$, restricting the choice of the renormalisation scale to $M_{0B} > M_{0L}$.

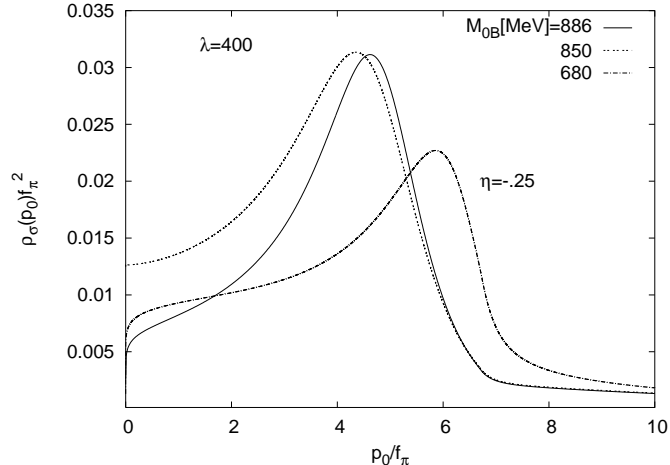


Fig. 3. The $T = 0$ spectral function for different allowed choices of M_{0B} and η in the chiral limit. The variation is restricted to the stability region of the system.

One finds from (20) $M_{0L} = m_{q0} \exp(\eta + 1)$ which, with our present numerical values of f_π and m_{q0} , gives $M_{0L} = 849.92$ MeV at $\eta = 0$ and $M_{0L} = 661.92$ MeV at $\eta = -0.25$. In the allowed region $M_{0B} < M_{0L}$, $|M_{Landau}|/|p_{0,pole}|$ stays always well above unity. There, the real part of the pole position and the maximum of the spectral function coincide as expected.

In Fig. 3 we display the emerging spectral functions for $M_{0B} = 850, 886$ MeV and $\eta = 0$. In addition also the curve for $M_{0B} = 680$ MeV and $\eta = -0.25$ is shown. The effect of the fermions brings the location of the “ σ -peak” closer to the phenomenologically expected region: at $\eta = 0$ we find $p_{0,peak} \leq 430$ MeV, while the corresponding poles are located at $\text{Re} p_{0,pole} \simeq 450$ MeV. The Γ_σ/M_σ ratios still turn out to be lower than expected by 40-50%. Finally, one might remark that the stability of the broken symmetry phase also imposes a lower limit on M_{0B} , which is, however, lower in our case than the bound, described above.

Two short notes are of order in connection with the thermal evolution of the poles. First, near T_c all “ σ -poles” flow to the origin of the p_0 plane asymptotically along the same curve. The real part of this trajectory scales with $\Phi(T)$, the imaginary part with $\Phi^2(T)$. This means that the inclusion of the fermions qualitatively changes the dynamics of the system, since in the pure $O(N)$ model the trajectory reached the origin along the imaginary axis. Second, for the scaling exponent of the order parameter, $\Phi(T) \sim (T - T_c)^\beta$, on the full second order line we find its mean field estimate $1/2$. For the single point of TCP $\beta = 1/4$ was found within the numerical accuracy of its determination, in full agreement with the standard result of statistical physics [26]. At TCP only logarithmic corrections are expected to this value.

5 Conclusions and discussion

In this letter we have presented a theoretically fully consistent derivation of the phase structure in the $T - \mu$ plane of strong matter from the chiral σ model in the chiral limit using an approximate solution valid to $\mathcal{O}(1/\sqrt{N})$ when the number of the Goldstone bosons (N) goes to infinity. A novel feature arising from including the fermions is the strong influence of the renormalisation scheme on the shape of the spectral function. It is essential to check also the dependence of the excitation spectra on the renormalisation scale, which allows to restrict considerably the range for the acceptable values of M_{0B} . The predictions on the phase boundary in the $T - \mu$ plane depend on the renormalisation scale(s) only smoothly, leading to a unique semi-quantitative characterisation of the phase structure. In the allowed range of the parameters one finds $T_c(\mu = 0)$ in reasonable agreement with the results of MC simulations, while one encounters a genuinely low value for $T_{TCP} \approx 60 - 70$ MeV.

Our approach can be further improved by the dynamical determination of the fermion mass from a one-loop Schwinger-Dyson equation. For a realistic comparison with hot heavy-ion systems it is important also to include the effect of explicit chiral symmetry breaking. Possible dependence on the renormalisation scheme can be optimised by requiring the best phenomenological description of the scalar-isoscalar spectral function for $T = 0$. These extensions require a careful implementation of the proposed (non-perturbative) renormalisation procedure, which will prove more complex than in the present case. Our final goal is the application of the large N method to the three-flavor $SU(3)_L \times SU(3)_R$ case with realistic constituent quark masses.

Acknowledgements

The authors acknowledge the support of the Hungarian Research Fund (OTKA) under contract numbers F043465, T034980, and T037689.

References

- [1] Z. Fodor and S.D. Katz, Phys. Lett. **B534** (2002) 87
- [2] Z. Fodor and S.D. Katz, JHEP 0203 (2002) 014
- [3] C.R. Allton *et al.*, Phys. Rev. **D66** (2002) 074507
- [4] P. de Forcrand and O. Philipsen, Nucl. Phys. **B642** (2002) 290
- [5] M. d’Elia and M.-P. Lombardo, Phys. Rev. **D67** (2003) 014505
- [6] S.D. Katz, *Lattice QCD at finite T and μ* , hep-lat/0310005

- [7] S. Chandrasekaran, M. Pepe, T.D. Steffen and U.-J.Wiese, *Non-linear Realisation of Chiral Symmetry on the Lattice*, hep-lat/0306020
- [8] F. Karsch, K. Redlich and A. Tawfik, Eur. J. Phys. **C29** (2003) 549
- [9] F. Karsch, K. Redlich and A. Tawfik, Phys. Lett. **B571** (2003) 67
- [10] A. Dumitru, D. Röder and J. Ruppert, hep-ph/0311119
- [11] A. Barducci, R. Casalbuoni, S. DeCurtis, R.Gatto and G. Pettini, Phys. Rev. **D49** (1994) 426
- [12] J. Berges and K. Rajagopal, Nucl. Phys. **B538** (1999) 215
- [13] O. Scavenius, Á. Mócsy, I.N. Mishustin and D.H. Rischke, Phys. Rev. **C64** (2001) 045202
- [14] H. Fujii, Phys. Rev. **D67** (2003) 094018
- [15] T. Hatsuda, T. Kunihiro and H. Shimizu, Phys. Rev. Lett. **82** (1999) 2840
- [16] J.I. Lenaghan and D.H. Rischke, J. Phys. **G26** (2000) 431; D. Röder, J. Ruppert and D.H. Rischke, Phys. Rev. **D68** (2003) 016003
- [17] J.C. Collins, *Renormalisation*, Cambridge University Press, 1987
- [18] J.-P. Blaizot, E. Iancu and U. Reinosa, Phys. Lett. **B568** (2003) 160
- [19] H. van Hees and J. Knoll, Phys. Rev. **D66** (2002) 025028
- [20] A. Patkós, Zs. Szép and P. Szépfalusy, Phys. Lett. **B537** (2002) 77
- [21] A. Patkós, Zs. Szép and P. Szépfalusy, Phys. Rev. **D66** (2002) 116004
- [22] L. Dolan and R. Jackiw, Phys. Rev. **D9** (1974) 3320
- [23] F. Karsch, E. Laermann and A. Peikeert, Nucl. Phys. **B605** (2001) 579
- [24] A. Ali Khan *et al.* [CP-PACS Collaboration] Phys. Rev. **D63** (2001) 034502
- [25] J. Cleymans and K. Redlich, Phys. Rev. **C60** (1999) 054908
- [26] W. Gebhardt and U. Krey, *Phasenübergänge und Kritische Phenomäne*, F. Vieweg & Sohn, Braunschweig, 1980